Enantiomer Separation in a Cascaded Micellar-Enhanced Ultrafiltration System

Pieter E. M. Overdevest, Marc H. J. Hoenders, Klaas van't Riet, and Albert van der Padt
Dept. of Agrotechnology and Food Science, Wageningen University and Research Center, 6700 EV Wageningen, The Netherlands

Jos T. F. Keurentjes
Dept. of Chemical Engineering, Eindhoven University of Technology, 5600 MB Eindhoven, The Netherlands

The increasing demand for optically pure compounds (enantiomers) stimulates the development of new enantiomer separation processes on an industrial scale. The separation of enantiomers by ultrafiltration of enantioselective micelles was studied in a cascaded system. The feasibility of this separation concept was proven by a cascade of five lab-scale units and a bench-scale system using an industrial membrane module. Model calculations show that the separation is not improved greatly at enantioselectivities (ratio of affinity constants) above 10 and the affinity of the enantioselective micelles for the substrate (enantiomers) plays a crucial role in the performance of the separation process. Modeling the separation as a function of the dimensionless affinity number (affinity constant · enantiomer feed concentration) shows that there is an operation window in which the separation satisfies its criterion of high yield and high enantiomeric excess. For countercurrent affinity systems, this implies that any research effort should focus on developing (microheterogeneous) media characterized by weak interactions with the substrate to allow for operation at high feed concentrations, not on high affinity systems.

Introduction

Since the biological activity of enantiomers can be different, the purity of these chiral compounds in pharmaceuticals, agrochemicals, and food additives is of crucial importance. Where one enantiomer has the desired activity, the mirror image of this compound can provoke negative side effects. Consequently, the development of new methods for the production of these optically pure compounds is encouraged by the industry.

A new separation technique, based on micelle-enhanced ultrafiltration (MEUF) (Scamehorn et al., 1989; Overdevest et al., 2000a), makes use of membranes in order to accomplish the separation of racemic mixtures (that is, an equimolar mixture of the two enantiomers). Membrane separations are attractive and cost-efficient, due to the possibility of continuous operation, low energy requirement, and ease of scale-up. The developed system contains nonionic micelles in which chiral selector molecules are anchored (de Bruin et al., 2000). Starting with a racemic mixture, the selector preferentially binds one of the two enantiomers. During ultrafiltration, the micelles are retained, including the bound enantiomers, while unbound enantiomers pass the membrane.

Equilibrium and kinetic models have been developed to describe the complexation of *D*,*L*-phenylalanine (*D*,*L*-Phe) enantiomers by cholesteryl-*L*-glutamate in nonionic micelles (Overdevest et al., 2000b, 2001b), which is our model system. A multistage system is under development that results in the separation of both enantiomers (Overdevest et al., 2000a) (Figure 1). If only one enantiomer is required at high purity, the other enantiomer can be reintroduced in the separation system after racemization. Then, the required number of stages will be less than in the case where both enantiomers are desired products. The objective of this article is to develop a model describing the separation in a multistage system, using the previously fitted complexation model (Overdevest et al., 2001a). Cascaded ultrafiltration experiments have

Correspondence concerning this article should be addressed to P. E. M. Overdevest.

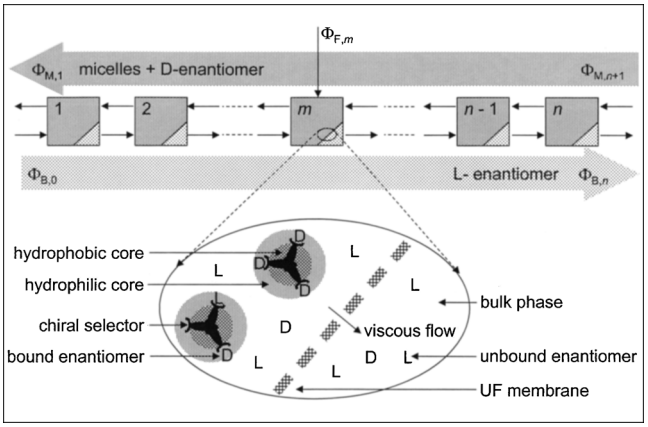

Figure 1. Cascaded system for the separation of racemic mixtures.

The cascaded process is operated in a countercurrent mode by moving the micellar phase and bulk phase in opposite directions through the system. Water enters stage 1, a racemate (equimolar solution of both enantiomers) enters stage m, and "empty" micelles enter the system in stage n. Under optimal conditions, the retentate of stage 1 is enriched with the D-enantiomer, where the permeate of stage n is enriched with the L-enantiomer. The oval in stage m is enlarged in the lower half of the figure showing the separation at a molecular level.

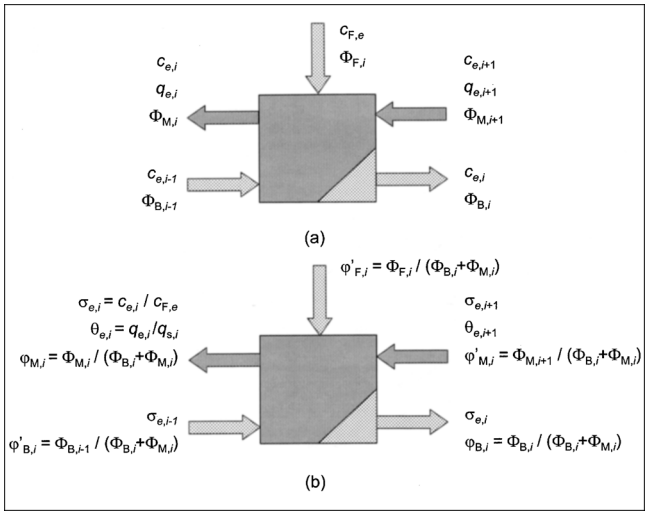

Figure 2. Single stage from the cascaded system: (a) dimensional variables, and (b) dimensionless numbers ($\Phi_{F,i\neq m}=0$, and $\varphi_{M,i}=1-\varphi_{B,i}$).

been conducted on both the lab and bench scale to validate the separation model. The lab-scale system consists of a series of five ultrafiltration (UF) units, while the bench-scale system is of only one single UF unit containing an industrial membrane module. In the bench-scale system the feed concentration is controlled to simulate the state of each UF stage in the multistage system.

Theory

Modeling the cascaded ultrafiltration system

Previously, we used multicomponent Langmuir isotherms to describe enantioselective equilibrium complexation (Overdevest et al., 2001a). Additionally, (de)complexation kinetics have been studied (Overdevest et al., 2001b). These models are now used to describe the enantiomer separation in a cascaded MEUF system of n stages (Figure 1). For each stage, mass balances are combined with the multicomponent isotherms. To avoid correlation between system parameters and input variables and to facilitate the scale-up of the separation system, dimensionless numbers are introduced (Figure 2; Appendix A)

$$I_i\frac{d(\sigma_{e,i}+\beta Q_i\theta_{e,i})}{d\theta}=\varphi'_{M,i}\sigma_{e,i+1}+\varphi_{M,i}\beta Q_i(\theta_{e,i+1}-\theta_{e,i})-\sigma_{e,i}+\varphi'_{F,i}+\varphi'_{B,i}\sigma_{e,i-1} \quad (1)$$

where $\sigma_{e,i}$ represents the dilution factor of enantiomer e (D or L) in the system, equal to the unbound enantiometer concentration in stage i, $c_{e,i}$ (mM), divided by the enantiomer feed concentration, $c_{F,e}$ (mM). The number β is a measure for the selector requirement: the selector concentration entering the cascade, $q_{s,F}$, divided by $c_{F,e}$. The mass flows through the system are characterized by their stage cut φ: the flow fraction of the sum of flows leaving (or entering) a stage. Both I_i and Q_i are functions of these stage cuts (see Appendix A).

At equilibrium, the bound enantiomer concentration $\theta_{e,i}$ is described by the Langmuir isotherms. Introducing the presented dimensionless parameters, these isotherms become

$$\theta_{D,i}=\frac{\alpha_{D/L,\mathrm{int}}\sigma_{D,i}}{1/\kappa_L+\alpha_{D/L,\mathrm{int}}\sigma_{D,i}+\sigma_{L,i}}$$
$$\theta_{L,i}=\frac{\sigma_{L,i}}{1/\kappa_L+\alpha_{D/L,\mathrm{int}}\sigma_{D,i}+\sigma_{L,i}} \quad (2)$$

where κ_L is the dimensionless affinity number for the L-enantiomer, equal to the affinity for this enantiomer K_L (mM^{-1}) times $c_{F,e}$. The intrinsic enantioselectivity $\alpha_{D/L,int}$ equals K_D over K_L. In case the residence time in the system is long enough to assume equilibrium (Overdevest et al., 2001b), the separation can be modeled using Eqs. 1 and 2. It should be noted that in this situation $d\theta_{e,i}/d\theta=(d\theta_{e,i}/d\sigma_{e,i})\cdot(d\sigma_{e,i}/d\theta)$. Otherwise, the complexation kinetics can be described by a linear driving force model (see Appendix B).

Optimization criterion and separation constraint

To optimize the separation process, both product yield and purity should be maximized using the minimum number of stages. In order to do so, a yield and purity constraint must be defined. For this cascaded system, we aim at a high purity of both the micellar phase leaving stage 1 and the bulk phase leaving stage n. Therefore, the sum of the enantiomeric excess in both phases, $ee_{sum}=ee_{M,1}+ee_{B,n}$ (%), should at least be equal to a chosen setpoint

$$\frac{ee_{\mathrm{sum}}}{100\%}=\frac{|q_{D,1}-q_{L,1}+c_{D,1}-c_{L,1}|}{q_{D,1}+q_{L,1}+c_{D,1}+c_{L,1}}+\frac{|c_{D,n}-c_{L,n}|}{c_{D,n}+c_{L,n}} \quad (3)$$

for example, a setpoint of 199% secures a high purity of both enantiomers ($\geq 99\%$). Thus, the high purity of both enantiomers leads to the high recovery of both enantiomers.

Extraction factor

The extraction factor, $\Lambda_{e,i}$, describes the ratio of the number of species, e, that leave separation stage, i, in the opposite directions (Alders, 1959) (Figure 2)

$$\Lambda_{e,i} = P_{e,i}\frac{1-\varphi_{B,i}}{\varphi_{B,i}} = \left(\frac{c_{e,i}+q_{e,i}}{c_{e,i}}\right)\frac{1-\varphi_{B,i}}{\varphi_{B,i}} \qquad (4)$$

where $P_{e,i}$ is the partition factor of an enantiomer in micellar and bulk phase, given by the Langmuir isotherms. Both $P_{e,i}$ and $\Lambda_{e,i}$ are useful tools in the development of the cascaded system, since it provides insight in how the separation can be improved. The extraction factors of the two enantiomers can be set opposite to unity by controlling the stage cuts $\varphi_{B,i}$, so that the D-enantiomers move effectively with the micellar phase ($\Lambda_{D,i} > 1$) and the L-enantiomers move in the opposite direction with the bulk phase ($\Lambda_{L,i} < 1$). Consequently, all $\varphi_{B,i}$ must be larger than 0.5.

Materials and Methods

Materials

We used nonionic micelles to prevent unfavorable nonselective ion-ion interactions between enantiomers and micelles. The nonionic surfactant, nonylphenyl polyoxyethylene [E10] ether (NNP 10), was a gift by Servo Delden b.v. (Delden, The Netherlands). The NNP 10 batch was a mixture of different NNPs, therefore, an average molecular weight of 644 g/mol was assumed. The chiral selector, cholesteryl-*L*-glutamate (CLG), was synthesized at the Department of Organic Chemistry (de Bruin et al., 2000). The optical rotation of the chiral selector $[\alpha]_D^{293}$ was $-27°$ at 10.5 g/L chloroform (3% trifluoracetic acid). The chiral selector contained a large hydrofobic anchor (cholesterol) to secure its solubility in the micelle. Throughout this study double distilled water was used. All other components were obtained from Merck (Darmstadt, Germany) and were used without further purification.

Preparation of micellar solutions

The micellar solutions were prepared as described previously (Overdevest et al., 2001a). The final solutions were set at pH 7 and contained 7.8 mM NNP10, 0.3 mM CLG, 0.3 mM $CuCl_2$, and 0.1 M KCl. To generalize terminology the Langmuir saturation concentration q_s refers to the effective chiral selector concentration.

Micelle-enhanced ultrafiltration in cascaded systems

Two types of experiments were conducted to validate the developed model for the separation of enantiomers in a cascaded system. First, a cascaded system that contained five stages was used. Second, one single-stage bench-scale system was used to simulate the separation in a cascaded system of 60 stages. Measurements of the enantiomer concentrations were performed by HPLC, as described previously (Overdevest et al., 2000b).

Cascaded System. As to the cascaded system shown in Figure 1, a five-stage system was operated in the countercurrent mode ($n = 5$). Each stage consisted of a stirred vessel with 0.5 L micellar solution and a hollow-fiber membrane module. A peristaltic pump (Watson Marlow 505S with 5 pump heads) was used to simultaneously pump the micellar solutions through five independent hollow-fiber cross-flow systems (Bio-Nephross Allegro dialyzers by Cobe Nephross BV) at 4.2×10^{-4} L/s. A second peristaltic pump with a multitube cassette (Watson Marlow 205U) pumped the permeate from membrane module i to micellar solution $i+1$, the flow rates $\Phi_{B,i}$ were 8.11×10^{-6} L/s for $0 \le i < m$ and 8.72×10^{-6} L/s for $m \le i \le n$ ($\varphi_{B1<i<m} = 0.700$ and $\varphi_{B,m\le i\le n} = 0.715$). The bulk phase that entered stage 1 contained 0.1 M KCl at pH 7. A second Watson Marlow 205U pumped the micellar solution from stage i to stage $i-1$, and the flow rate $\Phi_{M,i}$ was 3.47×10^{-6} L/s ($\varphi_{M,i} = 1-\varphi_{B,i}$). The micellar solution that entered the system in stage 5 was the same as was initially present in each stage. The racemic mixture fed to stage 4 ($m = 4$) at 6.08×10^{-7} L/s ($\varphi_{F,m} = 0.05$) contained 6 mM of *D,L*-Phe. The residence time in the membrane module (order of 3×10^2 s) can be neglected if compared to the residence time in each stage (4.3×10^4 s). Therefore, we could regard both flask and module as one single stage.

Samples were taken daily from both the permeate and micellar phase of each stage. It could be assumed that both nonselective enantiomer complexation by the nonionic surfactants and membrane rejection of unbound enantiomers can be neglected (Overdevest et al., 2000b). Therefore, in each stage the bound enantiomer concentration, $q_{e,i}$ (mM), could be calculated by subtracting the measured enantiomer concentration in the bulk phase, $c_{e,i}$ (mM), from the total concentration in the micellar phase. The total enantiomer concentration in the micellar phase was measured after diluting the 0.2-mL samples with 0.1 mL 2 M hydrochloric acid to provoke decomplexation. The cascade experiment was operated for 9×10^5 s at 4°C to avoid bacterial growth in the system. Plate counting of the micellar flow leaving stage 1 indeed showed that no contamination had occurred.

Bench-Scale System. Figure 3 depicts the cross-flow system used for the bench-scale ultrafiltration experiments (Amafilter b.v., Alkmaar, The Netherlands). The micellar solution was circulated at 0.125 L/s from a 10-L vessel through a spiral-wound membrane module containing a 1-m^2 cellulose membrane (Hoechst UF-C-10, 10 kDa MWCO) using a diaphragm pump (Wanner Engineering Inc., model D-10/G-

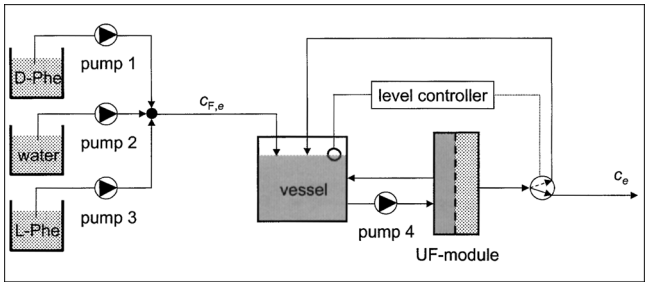

Figure 3. Bench-scale cross-flow system.

Pumps 1, 2 and 3 were PC controlled using Keithley's Testpoint software and I/O-card DDA-08/16 (Cleveland, OH). The vessel volume was kept at 10 L by an electronic level-controlled valve at the permeate side of the module. A Pharmacia fraction collector (Frac-100) continuously collected part of the permeate leaving this system.

10). The transmembrane pressure was set at 2×10^5 Pa, realizing a permeate flow of 5.56×10^{-3} L/s, which resulted in the permeate remaining in the module for under 3×10^2 s.

The equilibrium separation model (Appendix A, $\alpha_{D/L,\text{int}} = 1.9$, $\beta = 1$, $\kappa_L = 2.5$, so that $c_{F,e} = 0.28$ mM) was used to calculate the $c_{D,i}$ and $c_{L,i}$ profiles of Phe in a cascade of 60 stages, resulting in an ee_{sum} of 199%. The stage number of the single-stage bench-scale system in this cascaded system was simulated by controlling the feed concentrations of both enantiomers entering the bench-scale system, $c_{F,e}$. The feed concentrations of the bench-scale system were calculated using the equilibrium separation model, so that at steady state the unbound concentrations in the cascaded system equal the unbound concentration in the bench-scale system in time

$$c_{F,e} = c_e + \tau\frac{dc_e}{dt}\left(1+\frac{dq_e}{dc_e}\right), \quad \text{(mM)} \tag{5}$$

where c_e and dc_e/dt are derived from the calculated concentration profiles in the cascade, dq_e/dc_e is obtained from the Langmuir isotherms, and τ is the residence time of the bulk phase in the bench-scale system, which was set at 3.6×10^4 s. The equilibrium model (Eq. 5) would still result in a good approximation, comparing the residence time with the complexation kinetics (Overdevest et al., 2001b).

The concentration profiles could not be simulated by one single experiment within a time span of a few days, due to the discontinuity at the feeding stage of the cascade ($m = 35$). Therefore, two experiments were conducted, one simulating stage 1 to stage 35, the other started in stage 60 and stopped in stage 35.

After pump calibration, $c_{F,e}$ was related to the speed of pumps 1 and 3 (Figure 3). Water was added to the bench-scale system to maintain the total flow at a constant τ (pump 2)

Validation Experiments

Ultrafiltration experiments with a cascaded system

Design calculations show that extremely high enantioselectivities of around 10^4 are required to satisfy the separation constraint in one single stage. However, above a selectivity of 10 the separation hardly improves (Figure 4). A run with a five-stage ultrafiltration system has been conducted in order

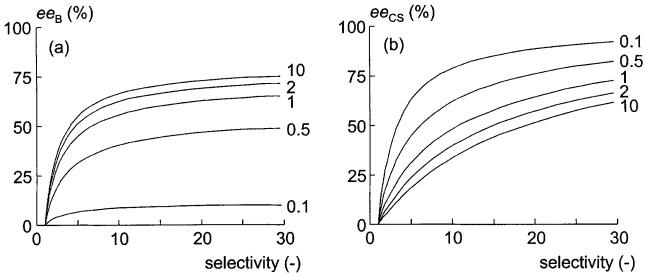

Figure 4. Enantiomer separation in a single stage for several ratios of selector and racemate concentrations.

(a) The *ee* in the bulk phase, $ee_B = |c_D - c_L|/(c_D + c_L)$; and (b) *ee* of enantiomers on chiral selectors, $ee_{CS} = |q_D - q_L|/(q_D + q_L)$.

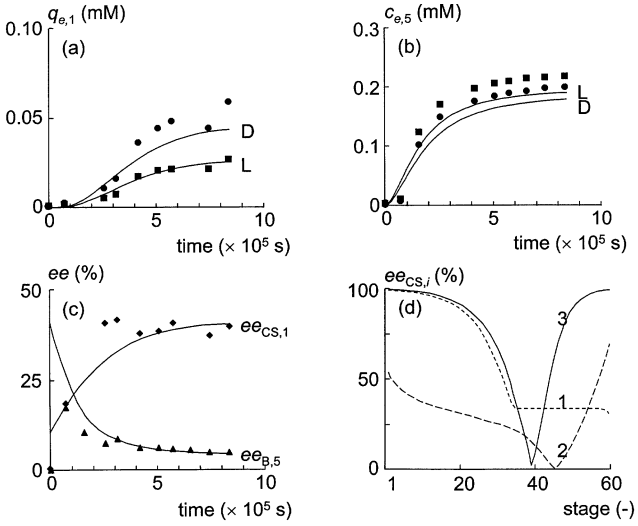

Figure 5. Ultrafiltration experiments in a cascade of 5 stages ($c_{F,e} = 3$ mM):

(a) Bound concentrations in stage 1 of *D*- (●) and *L*-Phe (■); (b) unbound concentrations in stage 5; (c) enantiomeric excess of (un)bound enantiomers, ee_B (▲) and ee_{CS} (◆); (d) ee_{CS} in a cascade of 60 stages under similar experimental conditions (dotted line 1), after process optimization (dashed line 2) and after additional medium optimization (solid line 3) (the solid lines in parts a, b, and c are equilibrium model predictions).

to validate the separation model (Eqs. 1 and 2). Figures 5a and 5b show the unbound and bound enantiomer concentrations leaving the cascade from stages 1 and 5, respectively. The preference of CLG for *D*-Phe causes, $q_{D,1}$, to exceed $q_{L,1}$ (Figure 5a). Consequently, the bulk phase is enriched with *L*-Phe (Figure 5b). The deviation between the measured and predicted unbound concentrations in stage 5 can be explained by just a 4% offset in the bulk phase flow. In spite of this minor deviation, the separation is well predicted ($ee_{B,5}$ in Figure 5c). Measuring and predicting an $ee_{CS,1}$ of 41% in a cascade of five stages (Figure 5c), calculations for one single stage have shown that under the same conditions an $ee_{CS,1}$ of only 27% is expected. Of course, $ee_{B,n}$ (4%) is not greatly influenced by the number of stages, when the feed stage is only one stage away from the outlet.

Despite the separation enhancement of the cascade as compared to one single stage, these measurements clearly show that five stages are still not sufficient to satisfy the constraint of $ee_{\text{sum}} > 199$ (Figure 5d). Dotted line 1 shows that these current experimental conditions can never lead to two optically pure products with any number of stages, where $\varphi_{B,1<i<m} = 0.700$ and $\varphi_{B,m\le i\le n} = 0.715$. In this case most enantiomers leave the system from stage n, due to the relatively high bulk-phase flow. Only a small amount leaves the system from stage 1 with high purity, of course. Therefore, the bulk-phase flow fractions of the total flow leaving each stage, $\varphi_{B,i} = \Phi_{B,i}/(\Phi_{B,i} + \Phi_{M,i})$, have been optimized in order to improve the separation. At the optimized set of $\varphi_{B,i}$, the relative transport of bound enantiomers increases, so that the separation improves at stage 60 and decreases at stage 1 (dashed line 2, $\varphi_{B,1<i<m} = 0.560$ and $\varphi_{B,m\le i\le n} = 0.575$). This shows that at a racemic mixture feed concentration of

6-mM optimization of the stage cuts alone is not enough to reach $99^+\%$ separation of both enantiomers. Engineering of the selective medium is needed to reduce the affinity of the chiral selector for the L-enantiomer from 8.9 to 0.83 mM^{-1} and increase the Langmuir saturation concentration from 0.17 to 3 mM to keep $c_{F,e}$ at 3 mM and still achieve that $ee_{sum} > 199\%$ (solid line 3). In dimensionless terms this implies that κ_L is reduced from 27 to 2.5 and β is increased from 0.057 to 1. An improved separation can also be achieved by diluting the system to $c_{F,e} = 0.28$ mM and $q_{s,n+1} = 0.28$ mM, keeping K_L at 8.9 mM^{-1}. All of these calculations have been performed using the experimentally determined $\alpha_{D/L,\text{int}} = 1.9$ (Overdevest et al., 2001a). Obviously, an increase in enantioselectivity reduces the required number of stages; this will be discussed in one of the following sections.

Cascade approximation by a single stage and calculated feed concentration strategy

Validating the model for 60 stages is hardly possible using the previously discussed lab-scale cascade setup. Hence, we have simulated a cascade of 60 stages using one single-stage ultrafiltration system by controlling the feed concentrations of both enantiomers, $c_{F,e}$ (mM). The position of the single-stage bench-scale system in the cascade can be approximated by a place-to-time transformation of the concentration profiles in the cascade. Therefore, the feed concentrations are chosen such that the expected unbound concentrations in the bench-scale system are equal to the calculated concentration profiles in the cascade corresponding to the solid line in Figure 5d.

Figure 6 shows the measured unbound concentrations of D- and L-Phe of the two independent experiments. The solid lines represent the expected concentrations using the kinetic model, including both the Langmuir isotherms and the linear driving-force model (Overdevest et al., 2001b). The minor difference between both model predictions is explained by the relatively long residence time as compared to the complexation kinetics. Since the measurement error is on the order of 0.002 mM, it is shown that both models describe the measurements well.

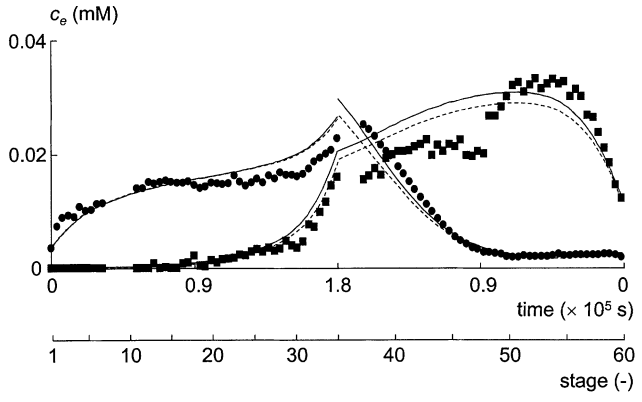

Figure 6. Ultrafiltration experiments in a bench-scale system simulating the separation of *D*- (●) and *L*-Phe (■) in a cascade of 60 stages.

The kinetic model predictions (solid lines) are not connected in stage 35, since the feed concentrations and the unbound concentrations have been calculated with different models, the equilibrium and kinetic model, respectively. The equilibrium model predictions are presented by the dotted lines. The deviation between model and measured data from stage 35 to 45 cannot be explained.

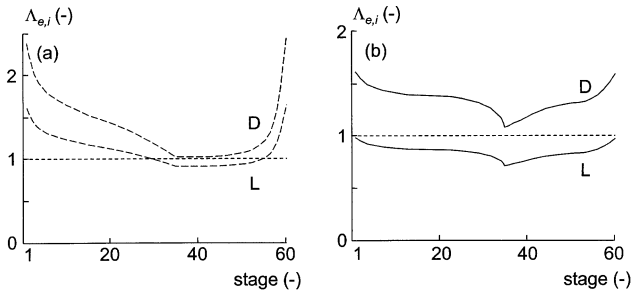

Figure 7. Extraction factors ($\Lambda_{e,i}$) in the 60 stage cascade.

(a) Corresponding to line 2 of Figure 5d dashed lines, $\kappa_L = 27$; [(b) corresponding to line 3 of Figure 5d solid lines, $\kappa_L = 2.5$]. The dotted line indicates $\Lambda_{e,i} = 1$, where $\Lambda_{L,i} < 1 < \Lambda_{D,i}$ for an effective separation process.

Extraction factors

The effect of κ_L on the separation performance of the cascade is shown by the extraction factors (Alders, 1959) in Figure 7. At high κ_L values it becomes apparent that nonlinear complexation behavior has a negative effect on the separation (Figure 7a). In this case, both enantiomers are transported in the same direction as the micellar phase. Sharply reducing κ_L (read K_L) causes the separation to become ineffective, $\Lambda_{L,i} = \Lambda_{D,i}$:

$$\lim_{K_L \downarrow 0} \Lambda_{e,i} = \lim_{K_L \downarrow 0} \left(\frac{c_{e,i} + q_{e,i}}{c_{e,i}} \right) \frac{1 - \varphi_{B,i}}{\varphi_{B,i}} = \frac{1 - \varphi_{B,i}}{\varphi_{B,i}} \quad (6)$$

Figure 7b shows $\Lambda_{e,i}$ at an optimized κ_L of 2.5, which implies a $c_{F,e}$ of 0.28 mM, since the affinity of CLG for L-Phe is 8.9 mM^{-1}.

The validation experiments have proven that the previously estimated Langmuir isotherms are suitable for describing the separation of phenylalanine enantiomers by our enantioselective micelles in cascaded ultrafiltration systems. Using the experimentally determined $\alpha_{D/L,\text{int}}$ of 1.9, model calculations show that 60 stages are sufficient to separate both enantiomers at $99^+\%$ purity. However, the enantiomer feed concentration of the cascade is in that case equal to 0.17 mM (that is, $\beta = 1$). The validated Langmuir equilibrium model will be used to maximize the enantiomer feed concentration and minimize the number of stages while satisfying the high purity constraint. This and the relations between the process and medium parameters and their effect on the productivity and purity are further discussed in the next section, using the defined dimensionless numbers.

System Optimization

The scope of this section is to indicate how the performance of cascaded ultrafiltration systems or any cascaded countercurrent nonlinear complexation system can be optimized. Therefore, we have analyzed the equilibrium model

and selected the dimensionless numbers effecting the separated by the cascade. Medium parameters ($\alpha_{D/L,\text{int}}$, β, and κ_L) describing the intrinsic properties of the enantioselective microheterogeneous medium are distinguished from process parameters (n and φ) that can be used to control the process at macroscopic scale:

$\alpha_{D/L,\text{int}}$ = D-enantiomer affinity constant/L-enantiomer affinity constant
β = selector feed concentration/enantiomer feed concentration
κ_L = L-enantiomer affinity constant · enantiomer feed concentration
n = number of stages
φ = flow in or out a stage/sum of flows in or out a stage.

These dimensionless numbers facilitate the elimination of a correlation between system parameters and input variables. The stage cuts (φ) have been optimized for a given set of medium parameters to minimize n under the constraint that the ee_{sum} ($= ee_{M,1} + ee_{B,n}$) exceeds the required enantiomeric excess. Depending on the undesirability of an impurity, this could be 199% or even 199.9%. In this section, the feeding stage (m) is chosen to be $n/2$ for all calculations. In addition, the implications of the optimized numbers will be discussed for both the model system and the competitive nonlinear complexation processes in general.

Parameters of the Medium

Affinity of microheterogeneous media for the substrate

To study the effect of κ_L on the separation performance of the cascaded system, ee_{sum} has been calculated as a function of this dimensionless affinity number (Figure 8a). These calculations show that there is a window where ee_{sum} complies with the optimization constraint. Below this κ_L window, the enantiomer concentrations of the micellar phase, $c_{e,i} + q_{e,i}$, and the bulk phase, $c_{e,i}$, become similar, which is cased by decreasing affinity, $q_{e,i} \to 0$ (Eq. 6). To explain the diminishing separation above the κ_L window, the total concentrations $q_{e,i} + c_{e,i}$ have been calculated for the cascade of 60 stages in Figure 8a at maximum ee_{sum}, where $\kappa_L = 2.5$ (Figure 8b). From these characteristic concentration profiles, it can be concluded that in the outer stages of the cascade the enantiomer concentrations are lower than in the center stages. The partition factor is constant for the linear extraction processes. The complexation behavior of the enantioselective micelles, however, is described by nonlinear Langmuir isotherms causing the partition factor, $P_{e,i} = (q_{e,i} + c_{e,i})/c_{e,i}$, to decrease when the concentration is increased. In other words, at both ends of the cascade, the micelles bind relatively more enantiomers, including the low-affinity substrate, in our case the L-enantiomer. Consequently, the extraction factor profiles are V-shaped (Figure 7). Note that $\varphi_{B,i}$ are constants at both ends of the feeding stage. Calculations show that the differences between $P_{D,i}$ and $P_{L,i}$ increase with κ_L. Above the κ_L window, the nonlinearity of $P_{e,i}$ increases to a level where it is impossible to correct all $P_{e,i}$ by a constant $\varphi_{B,i}$ to get all $\Lambda_{e,i}$ on opposite sides to unity. In agreement to our findings, Morbidelli et al., after studying both feed concentration and substrate affinity independently in simulated moving-bed units (Gentilini et al., 1998; Storti et al., 1995), have shown that complete separation occurs only in certain regions of flow ratios.

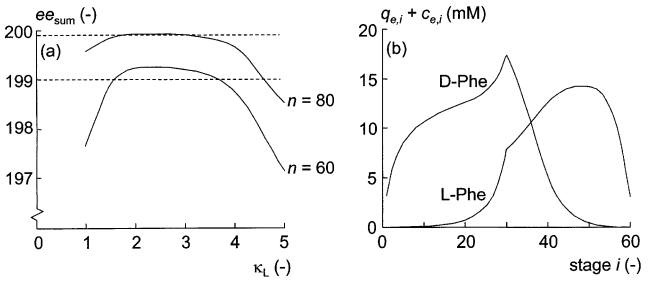

Figure 8. Cascade calculations using Langmuir equilibrium model, $\alpha_{D/L,\text{int}} = 1.9$.

(a) Effect of κ_L on cascade separation, ee_{sum} has been optimized for a range of κ_L using $\varphi_{B,i}$, where dotted lines represent $ee_{\text{sum}} = 199\%$ and 199.9%, respectively; (b) characteristic profiles of enantiomer concentrations ($n = 60$, $\kappa_L = 2.5$, $c_{F,e} = 40$ mM).

The existence of a κ_L window implies that a reduction in affinity improves the productivity of the cascaded system, since the racemic mixture feed concentration must be proportionally increased to maintain the optimal κ_L. Generally speaking, one can say that, in order to attain the highest possible feed concentration (that is, solubility concentration of the substrate) at $\alpha_{D/L,\text{int}} = 1.9$, the low-affinity constant (in our case K_L) should be 2.5 divided by the solubility of this substrate. The high-affinity constant is given by the low-affinity constant times $\alpha_{D/L,\text{int}}$. For our model system this implies that the affinity constants should decrease by a factor of 140, so that K_L becomes 0.063 mM^{-1} and the racemic mixture feed concentration can be increased to 80 mM (that is, solubility at 25°C). For CLG and D,L-Phe, the reduction in affinity can be reached by:

- Adjusting the hydrophobicity for the bulk phase to improve the preference of the enantiomers or the bulk phase (de Bruin et al., 2000; Overdevest and Van der Padt, 1999).
- Using a different ion to form the ternary complex. Cu^{II} ions are known to form very stable ternary complexes (Overdevest et al., 2001a; Brookes and Pettit, 1977). Ternary complexes based on Zn^{II}, Co^{II}, and Ni^{II} have a lower stability than complexes based on Cu^{II} (Allenmark, 1991).

Of course, one could also develop another selector, possibly based on nonionic interactions. The combination of an increased selector and racemate feed concentration and a decreased affinity increases the feasibility of an enantiomer separation process using enantioselective microheterogeneous media.

Process Parameters

In addition to medium and selector engineering approaches one could argue whether process engineering could offer alternatives. Therefore, we have studied the effect of the number of stages in the cascade n and the stage cuts of the bulk-phase flow $\varphi_{B,i}$.

Number of stages

Model calculations show that the width of the κ_L window depends on the enantioselectivity and the number of stages (Figure 8a). Its position is a direct result of the required ee_{sum} constraint. Toward process optimization, the κ_L windows have been calculated for two ee_{sum} constraints (199% and

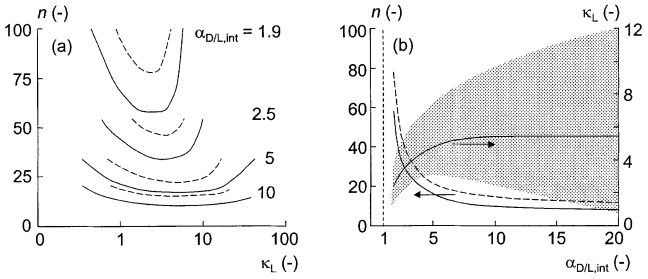

Figure 9. Cascade calculations using Langmuir equilibrium model.

(a) Required number of stages for a series of $\alpha_{D/L,int}$ and for an ee_{sum} of 199% (—) and 199.9% (– – –); (b) minimal number of stages (n) for an ee_{sum} of 199% (—) and 199.9%(– – –), and the coexisting value of κ_L. The gray area indicates κ_L, permitting the use of less than 5% more stages. The vertical dotted line represent $\alpha_{D/L,int} = 1$.

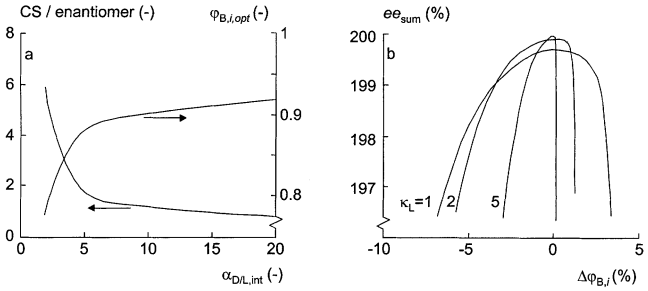

Figure 10. Cascade calculations using Langmuir equilibrium model.

(a) number of chiral selector molecules entering the cascade per enantiomer and the coexisting optimal stage cut of the bulk phase ($\varphi_{B,i,opt}$); (b) sensitivity of ee_{sum} for deviation in $\varphi_{B,i}$ from $\varphi_{B,i,opt}$.

199.9%) and a series of $\alpha_{D/L,int}$. 1.9 (experimentally measured for our model system), 2.5, 5, and 10 (Figure 9a). Based on the single-stage calculations, it is not expected that a further increase of $\alpha_{D/L,int}$ above 10 will reduce the number of stages required to fulfill the ee_{sum} constraint. The solid and dashed lines in Figure 9a represent the intersections of the curves and the dotted lines in Figure 8a, indicating an ee_{sum} of 199% and 199.9%, respectively, for a range of n. As expected, the required number of stages increases upon increasing ee_{sum} and upon a decreasing enantioselectivity. Furthermore, at low enantioselectivities the separation is more sensitive to the deviation in κ_L, caused by the smaller distance between the extraction-factor profiles of both enantiomers. Consequently, more stages are needed to balance this effect. The distance between the extraction profiles increases upon increasing enantioselectivity.

Optimization of the number of stages is performed by plotting the minima in Figure 9a as a function of the enantioselectivity (Figure 9b). Indeed, the decrease in the number of stages required to reach 199% or 199.9% separation diminishes at $\alpha_{D/L,int} > 10$. Moreover, the optimal κ_L increases upon enantioselectivity. However, overdesigning the cascade by less than 5% more stages makes a wide range of applicable κ_L values possible (gray area in Figure 9b).

Nevertheless, the number of stages alone is not sufficient to optimize the cascaded system. The costs of the system per kg of separated product should be minimized when ee_{sum} satisfies the required purity.

Stage cuts

The stage cuts $\varphi_{B,i} = \Phi_{B,i}/(\Phi_{B,i} + \Phi_{M,i})$ have a strong effect on the success of the separation in the cascade. This is also shown by Storti et al. for simulated moving-bed processes (Storti et al., 1993; Mazzotti et al., 1994). We have found that a $\varphi_{B,i}$ that is too high results in a migration of all enantiomers with the bulk phase, so that $ee_{M,1} = 100\%$ and $ee_{B,n} = 0\%$. The reverse is the case when $\varphi_{B,i}$ is too low ($ee_{M,1} = 0\%$ and $ee_{B,n} = 100\%$). Of course, in the cases where the $ee = 100\%$, there is no yield.

The optimal $\varphi_{B,i}$ increases with $\alpha_{D/L,int}$ (Figure 10a) and κ_L (not shown). Consequently, a larger membrane area per stage is required to separate the micelles from the bulk phase, On the other hand, the required number of stages decreases upon increasing $\alpha_{D/L,int}$. Hence, this should be optimized. Moreover, the required number of chiral selector molecules (CS) per enantiomer entering the cascade decreases, since $\varphi_{M,i} = 1 - \varphi_{B,i}$ at a constant β of 1.

Since stage cuts are an important factor in the separation performance of the cascaded system, pump stability should be guaranteed. Figure 10b shows that the sensitivity of ee_{sum} increases upon κ_L. As in our findings, Mazzotti et al. have calculated a decrease in robustness upon increasing the feed concentration (Mazzotti et al., 1997). The increased sensitivity at higher κ_L is also expressed by the V-shaped extraction factor profiles (see the subsection "Affinity of microheterogeneous media for the substrate"). Therefore, the $\Delta\varphi_{opt}$-window satisfying the ee_{sum} criterion, should be maximized to improve the robustness of the system.

The concentration difference over the stages in the cascade can be reduced (flatter extraction factor profiles) by a reflux, and therefore, improve the separation. It prevents the low-affinity enantiomer from leaving the system at stage 1 and helps leave the system at stage n. However, calculations ($n = 60$, $\alpha_{D/L,int} = 1.9$) show that the reflux ratios (Alders, 1959) of the high- and low-affinity enantiomers must be 2 and 10, respectively, to even out the concentration profiles, which results in large regeneration flows.

From Dimensionless Numbers to System Dimensions

In addition to the insight in the relation between the physical parameters describing the separation process, dimensionless numbers facilitate the scale-up of the separation process. For example, given one flow in the system, the dimensionless stage cuts relate this flow to all other flows in the system. Table 1 shows the necessary system dimensions to separate enantiomers at a certain rate.

It is concluded from case A that the low racemic mixture concentration results in large flows through the system, so that a large membrane area is required. Moreover, the system is very large (6.5 m^3 per stage) as a consequence of the slow complexation, 3×10^{-4} s^{-1} (Overdevest et al., 2001b). In addition to the extra costs of a larger apparatus, large amounts of chiral media are present in the apparatus (605 kg). Since it is expected that the chiral media will be the

Table 1. Required Cascade Dimensions to Separate 1 kg of Racemate per day*

	A	B
Productivity (kg/s)	$\mathbf{1.2\times10^{-5}}$	$\mathbf{1.2\times10^{-5}}$
Racemate feed (mM)	6.0	80††
Bulk phase flow into stage 1 (mL/s)	500	38
System membrane area (m^2)**	2.2×10^{3}	1.6×10^{2}
Complexation rate constant (s^{-1})	$\mathbf{3.0\times10^{-4}}$	0.18
Residence time per stage (s)	1.1×10^{4}	18
System volume (m^3)†	3.9×10^{2}	5.0×10^{-2}
Selector in system (kg)	6.1×10^{2}	**1**

Note: The required dimensions for an ee_{sum} of 199.32% have been calculated for two cases. Case A represents the conditions under which the cascaded experiments have been conducted using the model system. Case B represents a desired medium that, compared to the model system, (1) contains a higher selector concentration (40 mM), (2) has a lower affinity for the enantiomers (0.063 mM^{-1}), and (3) performs faster. Parameters in boldface have been fixed, others have been calculated using these constraints. For both cases: $n = 60$, $\alpha_{D/L,int} = 1.9$, $\kappa_L = 2.5$, $\beta = 1$, $\varphi_{B,1<i<m} = 0.775$, $\varphi_{B,m\le i\le n} = 0.779$.

**UF experiments resulted in a permeate flux of 14 mL/(m^2·s).

†Residence time = 3/complexation rate constant.

††Phe solubility at 25°C.

cost-determining factor of the separation system, it is desirable to improve the complexation kinetics. Note that the complexation rates of both Cu^{II} by hydroxyoximes in CTAB micelles (Cierpiszewski et al., 1996) and *D*,*L*-Phe by *N*-decyl-*L*-hydroxyproline in emulsion liquid membranes (Pickering and Chaudhuri, 1997) are only on the order of seconds. If the amount of selector in the system is restricted to 1 kg (equal to the amount of racemic mixture separated daily), it is necessary to increase the complexation rate to 0.18 s^{-1} (case B). Accordingly, each stage has a volume of approximately 1 L and requires a 2.7-m^2 membrane.

Since the complexation is not limited by diffusion (Overdevest et al., 2001b), it can be concluded that the complex formation itself is the rate-limiting factor in the complexation process. Selector engineering is the apparent instrument for developing faster complexation processes.

Concluding Remarks

This study clearly proves the suitability of microheterogeneous media (in our case micelles) in cascaded ultrafiltration systems for molecular separations. The separation of *D*,*L*-Phe by cholesteryl-*L*-glutamate can be adequately described by Langmuir isotherms. The validated separation model can be used to predict the number of stages necessary to reach high-purity products.

Model calculations show that the separation of enantiomers in a cascaded system is only successful within a certain κ-window (κ = enantiomer feed concentration multiplied by its affinity constant). Consequently, the productivity of the separation process can be improved by reducing the affinity of the microheterogeneous media for the enantiomers. Moreover, the contribution of a higher enantioselectivity to separation decreases sharply at enantioselectivities higher than 10. In addition, the desired increase in selector concentration from tenths of an mM to tens of an mM shows that, due to the reduction in specific surface area of the surfactant aggregates at higher surfactant concentrations, another medium must be applied. So, engineering of selective media should focus on the development of separation media characterized by a high selector concentration and weak interactions with enantiomers. For this, one should consider polymerized micelles or dendrimers.

Ultrafiltration of microheterogeneous media in cascaded systems utilizes the benefits of chromatographic and distillation processes: preferential binding under mild conditions and countercurrent flow of both the micellar phase and the bulk phase through the apparatus, respectively. Therefore, this concept provides a new basis for the development of large-scale separation techniques.

Acknowledgments

Financial support for this work was provided by the Dutch Technology Foundation (grant no. WCH44.3380), Akzo Nobel, and DSM.

Notation

$c_{e,i}$ = unbound concentration in stage i, mM
$c_{F,e}$ = enantiomer feed concentration (50% of racemate), mM
ee = enantiomeric excess, %
ee_{sum} = sum of $ee_{B,n}$ and $ee_{M,1}$, %
K_e = affinity constant, mM^{-1}
$k_{e,\pm1}$ = (de)complexation reaction rate constant, s^{-1}
$k_{DL,\pm1}$ = exchange reaction rate constant, $mM^{-1}\cdot s^{-1}$
n = number of stages
$q_{e,i}$ = bound enantiomer concentration in stage i, mM
$q_{s,i}$ = selector concentration in stage i, mM
$q_{s,F}$ = selector concentration in $\Phi_{M,n+1}$, mM
t = time, s
V_i = volume of micellar phase in stage i, L
$\Phi_{M,i}$ = flow of micellar phase leaving stage i, L/s
$\Phi_{B,i}$ = flow of bulk phase leaving stage i, L/s
$\Phi_{F,i}$ = flow of feed entering stage i, L/s
$[\alpha]_D^{293}$ = optical rotation at 293 K, using sodium emission spectrum (589 nm), deg
τ = residence time per stage, s

Dimensionless numbers

$\alpha_{D/L,int}$ = intrinsic selectivity, K_D/K_L
β = relative selector concentration, $q_{sF}/c_{F,e}$
ϵ = volume fraction of media particles in solution
$\varphi'_{M,i}$ = stage cut of micellar phase entering stage i, $\Phi_{M,i+1}/(\Phi_{B,i}+\Phi_{M,i})$
$\varphi_{M,i}$ = stage cut of micellar phase leaving stage i, $\Phi_{M,i}/(\Phi_{B,i}+\Phi_{M,i})$
$\varphi'_{B,i}$ = stage cut of bulk phase entering stage i, $\Phi_{B,i-1}/(\Phi_{B,i}+\Phi_{M,i})$
$\varphi_{B,i}$ = stage cut of bulk phase leaving stage i, $\Phi_{B,i}/(\Phi_{B,i}+\Phi_{M,i})$
$\varphi'_{F,m}$ = stage cut of feed entering stage m ($\varphi'_{F,i\neq m}=0$), $\Phi_{F,m}/(\Phi_{B,m}+\Phi_{M,m})$
I_i = reciprocal of relative sum of flows into stage i, $(\Phi_{B,1}+\Phi_{M,1})/(\Phi_{B,i}+\Phi_{M,i})$
κ_e = relative affinity, $K_e c_{F,e}$
$\Lambda_{e,i}$ = extraction factor in stage i, $P_{e,i}(1-\varphi_{B,i})/\varphi_{B,i}$
$P_{e,i}$ = partition factor in stage i, $(q_{e,i}+c_{e,i})/c_{e,i}$
Q_i = relative Langmuir saturation concentration in stage i, $q_{s,i}/q_{s,F}$
r_e = (de)complexation and exchange kinetics
$\sigma_{e,i}$ = dilution factor in stage i, $c_{e,i}/c_{F,e}$
$\theta_{e,i}$ = bound fraction in stage i, $q_{e,i}/q_{s,i}$
θ = relative time, $t\Phi_{T,1}/V_1$

A prime indicates a stage cut of flow entering a stage. The subscripts M, B, e, i, and m represent the micellar phase, the bulk phase, the *D*- or *L*-enantiomer, the stage number, and the feeding stage number, respectively.

Literature Cited

Alders, L., *Liquid-Liquid Extraction*, Elsevier, Amsterdam (1959).

Allenmark, S., *Chromatographic Enantioseparation*, Ellis Horwood, Chichester (1991).

Brookes, G., and L. D. Pettit, "Complex Formation and Stereoselectivity in the Ternary Systems Copper(II)–*D/L*-Histidine–*L*-Amino Acids," *J. Chem. Soc., Dalton Trans.*, 1918 (1977).

Cierpiszewski, R., M. Hebrant, J. Szymanowski, and C. Tondre, "Copper(II) Complexation Kinetics with Hydroxyoximes in CTAB Micelles. Effect of Extractant Hydrophobicity and Additives," *J. Chem. Soc. Dalton Trans.*, **92**, 249 (1996).

De Bruin, T. J. M., A.T. M. Marcelis, H. Zuilhof, L. M. Rodenburg, H. A. G. Niederlander, A. Koudijs, P. E. M. Overdevest, A. van der Padt, and E. J. R. Sudhölter, "Separation of Amino Acid Enantiomers by Micelle-Enhanced Ultrafiltration," *Chirality*, **12**, 627 (2000).

Gentilini A., C. Migliorini, M. Mazzotti, and M. Morbidelli, "Optimal Operation of Simulated Moving Bed Units for Nonlinear Chromatographic Separations: 2. Bi-Langmuir Isotherms," *J. Chromatogr. A*, **805**, 37 (1998).

Mazzotti, M., G. Storti, and M. Morbidelli, "Robust Design of Countercurrent Adsorption Separation Processes. 2. Multicomponent Systems," *AIChE J.*, **40**, 1825 (1994).

Mazzotti, M., G. Storti, and M. Morbidelli, "Optimal Operation of Simulated Moving Bed Units for Nonlinear Chromatographic Separations" *J. Chromatogr. A*, **769**, 3 (1997).

Overdevest, P. E. M., and A. Van der Padt, "Optically Pure Compounds from Ultrafiltration," *CHEMTECH*, **29**, 17 (1999).

Overdevest, P. E. M., J. T. F. Keurentjes, A. Van der Padt, and K. Van't Riet, "Resolution of Enantiomers Using Enantioselective Micelles in Ultrafiltration Systems," *Surfactant-Based Separations: Science and Technology*, *ACS Symp. Ser.*, **740**, American Chemical Society, Washington, DC, p. 123 (2000a).

Overdevest, P. E. M., A. Van der Padt, J. T. F. Keurentjes, and K. Van't Riet, "Langmuir Isotherms for Enantioselective Complexation of (*D/L*)-Phenylalanine by Cholesteryl-*L*-Glutamate in Nonionic Micelles," *Colloids Surf. A*, **163**, 209 (2000b).

Overdevest, P. E. M., T. J. M. DeBruin, E J. R. Sudhölter, K. Van't Riet, J, T. F. Keurentjes, and A. Van der Padt, "Separation of Racemic Mixture by Ultrafiltration of Enantioselective Micelles: 1. Effect of pH on Separation and Regeneration," *Ind. Eng. Chem. Res.*, **40**, 5991 (2001a).

Overdevest, P. E. M., M. A. I. Schutyser, T. J. M. De Bruin, K. Van't Riet, J. T. F. Keurentjes, and A. van der Padt, "Separation of Racemic Mixture by Ultrafiltration of Enantioselective Micelles: 2. (De)complexation Kinetics," *Ind. Eng. Chem. Res.*, **40**, 5998 (2001b).

Pickering, P. J., and J. B. Chaudhuri, "Equilibrium and Kinetic Studies of the Enantioselective Complexation of (*D/L*)-Phenylalanine with Copper(II) *n*-decyl-(*L*)-Hydroxyproline," *Chem. Eng. Sci*., **52**, 377 (1997).

Scamehorn, J. F., S. D. Christian, R. T., Ellington, *Surfactant-Based Separation Processes*, Dekker, New York (1989).

Storti, G., M. Mazzotti, M. Morbidelli, and S. Carrà, "Robust Design of Binary Countercurrent Adsorption Separation Processes," *AIChE J*., **39**, 471 (1993).

Storti, G., R. Baciocchi, M. Mazzotti, and M. Morbidelli, "Design of Optimal Operating Conditions of SMB Adsorptive Separation Units," *Ind. Eng. Chem. Res.*, **34**, 288 (1995).

Appendix A

The separation in a cascade of ultrafiltration stages is modeled by n mass balances to describe the total enantiomer concentration, $c_{e,i} + q_{e,i}$ (mM), of each enantiomer, e, in the micellar phase of each stage, i (Figure 2)

$$V_i\left(\frac{dc_{e,i}}{dt} + \frac{dq_{e,i}}{dt}\right) = \Phi_{M,i+1}(c_{e,i+1} + q_{e,i+1}) - \Phi_{M,i}(c_{e,i} + q_{e,i}) + \Phi_{F,i}c_F + \Phi_{B,i-1}c_{e,i-1} - \Phi_{B,i}c_{e,i} \quad \text{(mol/s)}$$

where $c_{e,i}$ and $q_{e,i}$ are the unbound and bound enantiomer concentrations, respectively; V (L) is the volume of the micellar phase; and Φ (L/s) represents the various mass flows through the system. Normalizing the concentrations to the enantiomer feed concentration, $c_{F,e}$ (mM)

$$V_i\left(\frac{d\sigma_{e,i}}{dt} + \beta Q_i\frac{d\theta_{e,i}}{dt}\right) = \Phi_{M,i+1}(\sigma_{e,i+1} + \beta Q_{i+1}\theta_{e,i+1}) - \Phi_{M,i}(\sigma_{e,i} + \beta Q_i\theta_{e,i}) + \Phi_{F,i} + \Phi_{B,i-1}\sigma_{e,i-1} - \Phi_{B,i}\sigma_{e,i} \quad \text{(L/s)}$$

where $\sigma_{e,i}$ is the unbound concentration relative to $c_{F,e}$; $\theta_{e,i}$ is the fraction of occupied selectors; β is the ratio of the selector concentration entering the cascade in stage n $q_{s,F}$ (mM) and $c_{F,e}$; and Q_i is the ratio of the selector concentration in stage i $q_{s,i}$ (mM) and $q_{s,F}$. Since, $\Phi_{M,i+1}Q_{i+1} = \Phi_{M,i}Q_i$

$$V_i\left\{\frac{d\sigma_{e,i}}{dt} + \beta Q_i\frac{d\theta_{e,i}}{dt}\right\} = \Phi_{M,i+1}\sigma_{e,i+1} + \Phi_{M,i}\beta Q_i(\theta_{e,i+1} - \theta_{e,i}) - (\Phi_{M,i} + \Phi_{B,i})\sigma_{e,i} + \Phi_{F,i} + \Phi_{B,i-1}\sigma_{e,i-1}. \quad \text{(L/s)}$$

Introducing the dimensionless stage cuts φ

$$I_i\left\{\frac{d\sigma_{e,i}}{d\theta} + \beta Q_i\frac{d\theta_{e,i}}{d\theta}\right\} = \varphi'_{M,i}\sigma_{e,i+1} + \varphi_{M,i}\beta Q_i(\theta_{e,i+1} - \theta_{e,i}) - \sigma_{e,i} + \varphi'_{F,i} + \varphi'_{B,i}\sigma_{e,i-1} \quad \text{(A1)}$$

where the prime indicates the stage cut of a flow entering a stage, and I_i is the ratio of the sum of flows into stage 1 and the sum of flows into stage i.

Appendix B

The complexation kinetics have been thoroughly investigated in a previous paper (Overdevest et al., 2001b). According to the kinetic complexation model, the bound enantiomer concentration in stage i $q_{e,i}$ (mM) cannot be directly calculated using the Langmuir isotherms and the unbound concentrations in stage i $c_{e,i}$ (mM). Therefore, mass balances for both unbound and bound enantiomers must be differentiated. Following a similar approach as in Appendix A, these mass balances are

$$I_i\frac{d\sigma_{e,i}}{d\theta} = \varphi'_{B,i}\sigma_{e,i-1} - \sigma_{e,i} + \varphi'_{M,i}\sigma_{e,i+1} + \varphi_{F,i} - r_e$$

$$I_i\frac{d\theta_{e,i}}{d\theta} = \varphi_{M,i}(\theta_{e,i+1} - \theta_{e,i}) + \frac{r_e}{\beta Q_i}$$

where r_e is the kinetic term representing the complexation, decomplexation, or exchange process. For complexation ($\theta_{e,i} > \theta_{\text{eq},e,i}$)

$$r_e = k_{e,+1}\tau_i(\sigma_{e,i} - \sigma_{eq,e,i})$$

For decomplexation ($\theta_{e,i} > \theta_{eq,e,i}$)

$$r_e = -k_{e,-1}\tau_i \beta Q_i(\sigma_{e,i} - \sigma_{eq,e,i})$$

And for exchange ($\sigma_{D,i} > \sigma_{\mathrm{eq},D,i} \wedge \theta_{L,i} > \theta_{\mathrm{eq},L,i}$)

$$r_D = k_{D,+1}\tau_i(\sigma_{D,i} - \sigma_{\mathrm{eq},D,i}) + k_{DL,+1}\tau_i \beta Q_i c_F(\sigma_{D,i} - \sigma_{\mathrm{eq},D,i})(\theta_{L,i} - \theta_{\mathrm{eq},L,i})$$

$$r_L = -k_{L,-1}\tau_i \beta Q_i(\theta_{L,i} - \theta_{\mathrm{eq},L,i}) - k_{DL+1}\tau_i \beta Q_i c_F(\sigma_{D,i} - \sigma_{\mathrm{eq},D,i})(\theta_{L,i} - \theta_{\mathrm{eq},Li,i})$$

The Langmuir isotherms are used to calculate the unbound and bound enantiomer concentrations in stage i ($c_{\mathrm{eq},e,i}$ and $\theta_{\mathrm{eq},e,i}$) in equilibrium with the actual bound and unbound enantiomer concentrations, respectively (Overdevest et al., 2001b).

Manuscript received Dec. 22, 2000, and revision received Feb. 6, 2002.